

# Parity reversion of ${}_{\Lambda}^{12}\text{Be}$

H. Homma<sup>1</sup>, M. Isaka<sup>1</sup> and M. Kimura<sup>2</sup>

<sup>1</sup>*Department of CosmoSciences, Graduate School of Science,*

*Hokkaido University, Sapporo 060-0810, Japan*

<sup>2</sup>*Creative Research Institution (CRIS),*

*Hokkaido University, Sapporo 001-0021, Japan*

## Abstract

The spectrum of  ${}_{\Lambda}^{12}\text{Be}$  is studied by an extended version of antisymmetrized molecular dynamics for hypernuclei. The result predicts the positive-parity ground state of  ${}_{\Lambda}^{12}\text{Be}$  that is reverted to the normal one by the impurity effect of  $\Lambda$  particle. The reversion of the parity is due to the difference of  $\Lambda$  binding energy in the positive- and negative-parity states that originates in the difference of  $\alpha$  clustering and deformation.

Despite of their short lifetime, hypernuclei have been a subject of particular interest in nuclear physics. They provide an almost unique opportunity to investigate underlying baryon-baryon interactions. Especially the knowledge of the interaction between  $\Lambda$  and nucleons is greatly increased in these decades [1–6]. This development strongly promotes the physics of hypernuclear many-body problems. A peculiar interest of hypernuclear many-body problems is the dynamical features  $\Lambda$  hypernuclei manifest by the addition of  $\Lambda$  particle such as the stabilization of the system [7, 8], modifications of sizes [9, 10], deformation and clustering [11–16]. Thus, hypernuclear many-body physics can be regarded as an impurity physics. It offers a means to investigate dynamical responses of nuclei to the addition of hyperons or a means to investigate nuclear structure by using hyperons as probe. As the forthcoming experiments will expand domain of hypernuclear physics to neutron-rich or heavier system, many exotic phenomena due to the impurity effect of  $\Lambda$  will be uncovered.

Single  $\Lambda$  hypernuclei of neutron-rich Be isotopes are one of such systems of interest and to be experimentally accessible. More specifically,  ${}_{\Lambda}^{12}\text{Be}$  is of particular interest, since the core nucleus  ${}^{11}\text{Be}$  is known to have quite exotic structure. It has two bound states with positive- and negative-parity. The ground state is positive parity and the negative-parity state is located at 320 keV above the ground state [17–19]. Since the order of these two states contradicts to the ordinary nuclear shell ordering and the neutron shell gap of  $N = 8$  is collapsed, it is called “parity inversion” and “breakdown of  $N = 8$  magic number”. Our question is how the “parity reversion” will be affected and modified in  ${}_{\Lambda}^{12}\text{Be}$  by the impurity effect of  $\Lambda$ . This letter reports that the parity inverted in  ${}^{11}\text{Be}$  will be reverted in  ${}_{\Lambda}^{12}\text{Be}$  by adding  $\Lambda$  particle. This study is based on the theoretical framework of antisymmetrized molecular dynamics (AMD). AMD has been applied to investigate the exotic phenomena in neutron-rich nuclei and has successfully described them such as the breakdown of  $N = 8$  and  $N = 20$  magic numbers [20–25]. In this study, we use an extended version of AMD for hypernuclei (HyperAMD) to investigate  ${}_{\Lambda}^{12}\text{Be}$ . HyperAMD has already been applied to  $p$ - $sd$  shell hypernuclei [15, 16] and the reader is directed to them for its detailed formulation. The Hamiltonian used in this study is given as,

$$H = H_N + H_{\Lambda} - T_g, \quad (1)$$

$$H_N = T_N + V_{NN} + V_C, \quad H_{\Lambda} = T_{\Lambda} + V_{\Lambda N}, \quad (2)$$

where  $T_N, T_{\Lambda}$  and  $T_g$  are the kinetic energies of the nucleons,  $\Lambda$  particle and the center-

of-mass motion. The Gogny D1S [26] is used as an effective nucleon-nucleon interaction  $V_{NN}$ , and the Coulomb interaction  $V_C$  is approximated by the sum of seven Gaussians. To see the dependence on  $\Lambda N$  interaction, a couple of  $\Lambda N$  effective interactions  $V_{\Lambda N}$  are examined. We have used  $YN$  G-matrix interactions YNG-ND and YNG-NF [2] which are respectively derived from the realistic one-boson-exchange potentials of the Nijmegen model-D and model-F [1]. We also used a modified version of YNG-NF (Improved-NF) suggested by Hiyama *et al.* [27]. These  $\Lambda N$  interactions have the dependence on the nucleon Fermi momentum  $k_F$  and the value of  $k_F = 0.973 \text{ fm}^{-1}$  is applied, that is common to the Ref. [27].

The variational wave function of HyperAMD is the eigenstate of the parity. The intrinsic wave function  $\Psi_{int}$  is represented by the direct product of the  $\Lambda$  single particle wave function  $\varphi_\Lambda$  and the wave function of the  $A$  nucleons  $\Psi_N$  which is a Slater determinant of the nucleon wave packets  $\psi_i$ ,

$$\Psi^\pm = P^\pm \Psi_{int}, \quad \Psi_{int} = \Psi_N \otimes \varphi_Y, \quad (3)$$

$$\Psi_N = \frac{1}{\sqrt{A!}} \det\{\psi_i(\mathbf{r}_j)\}, \quad (4)$$

where  $P^\pm$  is the parity projector. The nucleon single particle wave packet is represented by a Gaussian,

$$\psi_i(\mathbf{r}) = \phi_i(\mathbf{r}) \chi_i \tau_i, \quad (5)$$

$$\phi_i(\mathbf{r}) = \prod_{\sigma=x,y,z} \left( \frac{2\nu_\sigma}{\pi} \right)^{1/4} \exp\{-\nu_\sigma (r - Z_i)_\sigma^2\}, \quad (6)$$

$$\chi_i = a_i \chi_\uparrow + b_i \chi_\downarrow, \quad \tau_i = \text{p or n.} \quad (7)$$

The  $\Lambda$  single particle wave function is represented by a sum of Gaussians,

$$\varphi_\Lambda(\mathbf{r}) = \sum_{m=1}^M c_m \varphi_m(\mathbf{r}), \quad \varphi_m(\mathbf{r}) = \phi_m(\mathbf{r}) \chi_m, \quad (8)$$

$$\phi_m(\mathbf{r}) = \prod_{\sigma=x,y,z} \left( \frac{2\nu_\sigma}{\pi} \right)^{1/4} \exp\{-\nu_\sigma (r - \zeta_m)_\sigma^2\}, \quad (9)$$

$$\chi_m = \alpha_m \chi_\uparrow + \beta_m \chi_\downarrow, \quad (10)$$

where the number of Gaussians  $M$  is chosen large enough to achieve the energy convergence. The centroids of Gaussian wave packets  $\mathbf{Z}_i$  and  $\boldsymbol{\zeta}_m$ , the width of Gaussian  $\nu_\sigma$ , the coefficients  $c_m$  and spin directions  $a_i, b_i, \alpha_m, \beta_m$  are the variational parameters. They are so determined

to minimize the total energy under the constraint on the matter quadrupole deformation parameter  $\beta$  [20]. The constraint is imposed on the value of  $\beta$  from 0 to 1.2 with the interval of 0.025.

After the variation, we project out the eigenstate of the total angular momentum  $J$  for each value of  $\beta$ ,

$$\Psi_{MK}^{J\pm}(\beta) = \frac{2J+1}{8\pi^2} \int d\Omega D_{MK}^{J*}(\Omega) R(\Omega) \Psi^\pm(\beta). \quad (11)$$

The integrals over three Euler angles  $\Omega$  are performed numerically. The calculation is completed by the generator coordinate method (GCM) [28]. The wave functions that have different values of  $K$  and  $\beta$  are superposed,

$$\Psi_n^{J\pm} = \sum_p \sum_{K=-J}^J c_{npK} \Psi_{MK}^{J\pm}(\beta_p). \quad (12)$$

The coefficients  $c_{npK}$  are determined by solving Griffin-Hill-Wheeler equation.

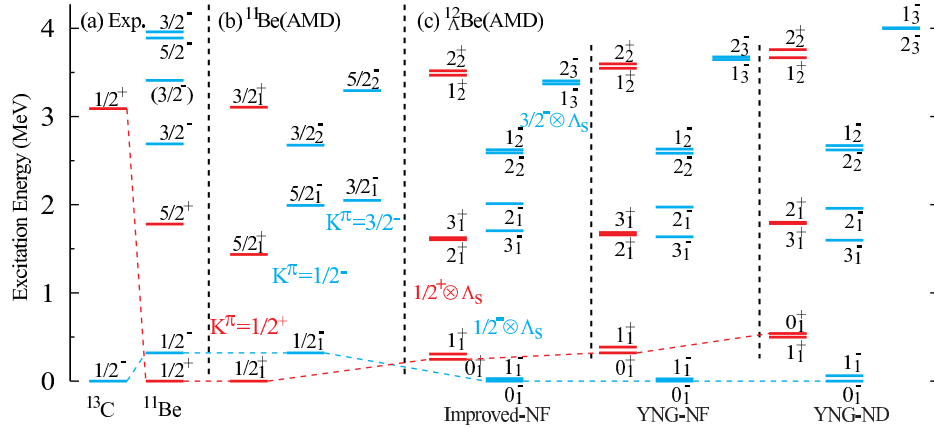


FIG. 1: (color online) (a) Observed spectra of  $^{13}\text{C}$  and  $^{11}\text{Be}$ . (b) Spectrum of  $^{11}\text{Be}$  calculated by AMD. (c) Spectra of  $^{12}_{\Lambda}\text{Be}$  calculated by HyperAMD with three different  $\Lambda N$  interactions.

Before the discussion on  $^{12}_{\Lambda}\text{Be}$ , it is helpful to overview the structure of  $^{11}\text{Be}$ . Figure 1 (a) shows the observed spectra of  $N = 7$  isotones,  $^{13}\text{C}$  and  $^{11}\text{Be}$ . The large shell gap between  $p_{1/2}$  and  $sd$ -shell in  $^{13}\text{C}$  is collapsed in  $^{11}\text{Be}$ . Namely, the ground state is positive parity and the order of  $p_{3/2}$  and  $sd$ -shell looks inverted in  $^{11}\text{Be}$ , that is called “parity inversion” [17, 18]. Using the original parameter set of the Gogny D1S, our calculation successfully reproduces the spin-parity of the ground state with the binding energy of 65.32 MeV and the first excited state  $1/2^-_1$  is located at 540 keV, while the observed values are 65.48 MeV

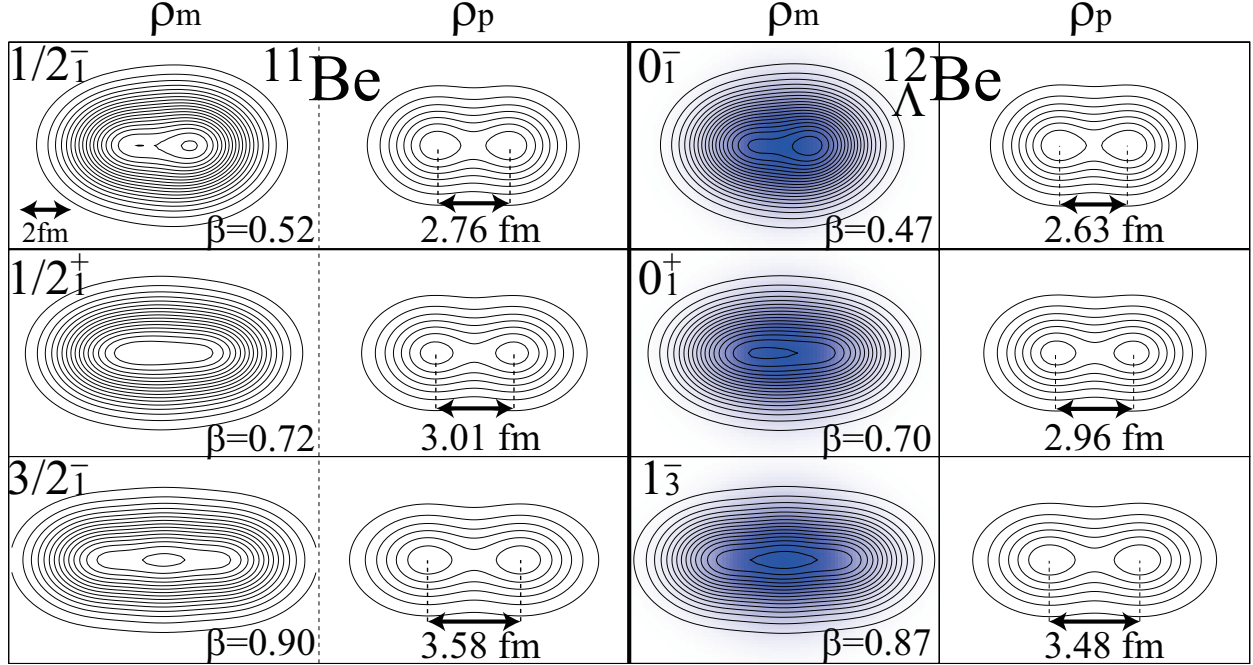


FIG. 2: (color online) Matter ( $\rho_m$ ) and proton ( $\rho_p$ ) density distributions of the each band head states of  $^{11}\text{Be}$  and  $^{12}_{\Lambda}\text{Be}$ . Color plots show the density distribution of  $\Lambda$  particle.

and 320 keV, respectively [19]. For more quantitative discussion of  $^{12}_{\Lambda}\text{Be}$ , we have weakened the spin-orbit interaction of Gogny D1S by 5% to reproduce the observed  $1/2^-$  excitation energy exactly. By this modification, the binding energy of  $^{11}\text{Be}$  is calculated as 64.77 MeV and the resulting spectrum is shown in Fig. 1 (b). Here, the excited unbound states are calculated within the bound state approximation.

It is known that the low-lying states of Be isotopes have  $2\alpha$  cluster core and valence neutrons occupying the molecular-orbits around the core which are so-called  $\pi$  and  $\sigma$  orbits [22]. The formation of the  $2\alpha$  cluster core in each state is confirmed in the proton density shown in Fig. 2. The ground state is a member of the  $K^\pi = 1/2^+$  band in which two of three valence neutrons occupy  $\pi$ -orbit and the last valence neutron occupies  $\sigma$ -orbit. In terms of the spherical shell model, a neutron is promoted into  $sd$ -shell across the  $N = 8$  shell gap (breakdown of magic number  $N = 8$ ). The first excited state is negative parity and belongs to the  $K^\pi = 1/2^-$  band. All valence neutrons occupy  $\pi$ -orbit or  $p$ -shell, that corresponds to the normal shell order. As we can see in Fig. 2 and Table I, the ground state has more pronounced  $2\alpha$  clustering and larger quadrupole deformation  $\beta$  than the first excited state. Here, deformation  $\beta$  of each state is defined as that of the basis wave function  $\Psi_{MK}^{J\pm}(\beta)$  which

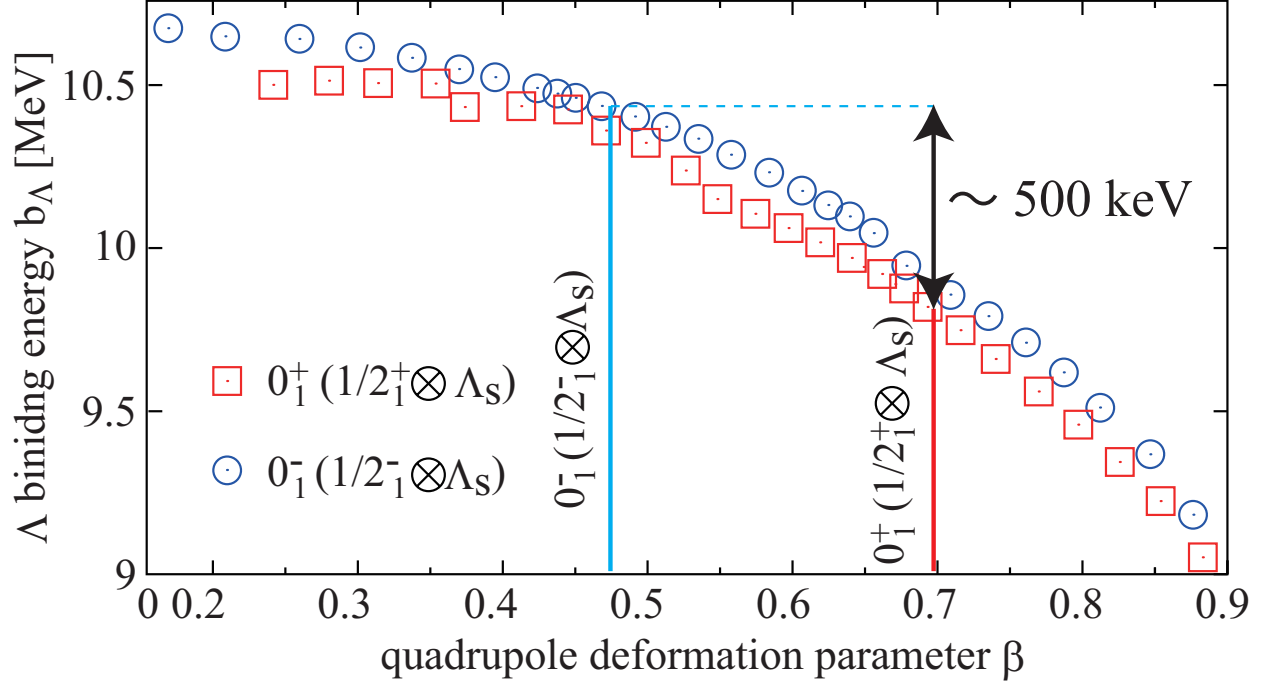


FIG. 3: (color online) The  $\Lambda$  binding energy of the  $0_1^-$  and  $0_1^+$  states as function of proton quadrupole deformation parameter  $\beta$ . Lines in the figure denote the deformation parameter of  $0_1^\pm$  states given in Table. I

has the maximum overlap with the GCM wave function (Eq. 12). The  $3/2_2^-$  state (band head of  $K^\pi = 3/2^-$ ) that has two valence neutrons in  $\sigma$ -orbit is most deformed amongst the band-head states. Including the  $3/2_2^-$  state, the assignment of the unbound excited states is still under discussion, and we devote further discussions to the Refs. [30–32]. We just remark here that the ground state is more deformed than the first excited state and has a neutron in  $sd$ -shell.

The spectra of  ${}_{\Lambda}^{12}\text{Be}$  obtained with three different  $\Lambda N$  interactions are shown in Fig. 1 (c). All states shown in the figure have a  $\Lambda$  in  $s$ -orbit and are classified into three bands. They are generated by the coupling of  $K^\pi = 1/2^+, 1/2^-$  and  $3/2^-$  bands of  ${}^{11}\text{Be}$  with  $\Lambda$  in  $s$ -orbit, and therefore, there are always doublet states of  ${}_{\Lambda}^{12}\text{Be}$  for each corresponding state of  ${}^{11}\text{Be}$ . These bands are denoted as  $K^\pi = 1/2^+ \otimes \Lambda_s, 1/2^- \otimes \Lambda_s$  and  $3/2^- \otimes \Lambda_s$ .

It is found that all of three  $\Lambda N$  interactions predicts the negative-parity ground state and give qualitatively same results. Therefore, we focus on the Improved-NF result for a while. The ground doublet is the  $0_1^-$  and  $1_1^-$  states with the binding energies of 74.69 and 74.66 MeV, that have the configuration of  ${}^{11}\text{Be}(1/2_1^-) \otimes \Lambda_s$ . The first excited doublet is  $0_1^+$  and

TABLE I: Calculated binding and excitation energies  $B$  and  $E_x$  [MeV], matter quadrupole deformation  $\beta$  and root-mean-square radii  $r_{rms}$  [fm] for band-head states of  $^{11}\text{Be}$  and  $^{12}_{\Lambda}\text{Be}$ . Numbers in parenthesis shows the observed data [29]. The  $\Lambda$  binding energy  $B_{\Lambda}$  [MeV], the of  $\Lambda$  kinetic energy  $T_{\Lambda}$  [MeV] and  $\Lambda N$  potential energy  $V_{\Lambda N}$  [MeV] are also shown for  $^{12}_{\Lambda}\text{Be}$ .

	$J^{\pi}$	$B$	$E_x$	$\beta$	$r_{rms}$	$B_{\Lambda}$	$T_{\Lambda}$	$V_{\Lambda N}$
	$1/2_1^-$	64.45	0.32	0.52	2.53			
		(65.16)	(0.32)					
$^{11}\text{Be}$	$1/2_1^+$	64.77	0	0.72	2.69			
		(65.48)	(0)		(2.73)			
	$3/2_1^-$	62.72	2.05	0.90	2.98			
	$0_1^-$	74.69	0	0.47	2.51	10.24	6.71	-16.93
$^{12}_{\Lambda}\text{Be}$	$0_1^+$	74.44	0.25	0.70	2.67	9.67	6.68	-16.42
	$1_3^-$	71.32	3.37	0.87	2.94	8.60	6.36	-15.08

$1_1^+$  states at 250 and 310 keV with the configuration of  $^{11}\text{Be}(1/2_1^+) \otimes \Lambda_s$ . Thus the ground state parity is reverted in  $^{12}_{\Lambda}\text{Be}$ , as if the addition of  $\Lambda$  has restored the  $N = 8$  shell gap. This parity reversion of  $^{12}_{\Lambda}\text{Be}$  is due to the difference of  $\Lambda$  binding energy  $B_{\Lambda}$  in the ground and first excited doublets. As shown in Table. I, the  $0_1^-$  state has larger  $B_{\Lambda}$  than the  $0_1^+$  state by about 500 keV. Here  $B_{\Lambda}$  is defined as the difference of binding energies between  $^{12}_{\Lambda}\text{Be}$  and corresponding  $^{11}\text{Be}$  states,

$$B_{\Lambda} = B(^{12}_{\Lambda}\text{Be}(J^{\pi})) - B(^{11}\text{Be}(J^{\pi})). \quad (13)$$

The change of the nuclear part  $H_N$  by addition of  $\Lambda$  is rather small. Therefore the difference of  $B_{\Lambda}$  overwhelms the energy difference between the  $1/2_1^{\pm}$  states of  $^{11}\text{Be}$ , and the parity reversion is realized in  $^{12}_{\Lambda}\text{Be}$ . The difference in  $B_{\Lambda}$  mainly comes from the difference in the  $\Lambda N$  potential  $V_{\Lambda N}$  as shown in Table. I, and it originates in the difference of the quadrupole deformation. Figure 3 shows the  $\Lambda$  binding energies in  $0_1^{\pm}$  states as function of quadrupole deformation, that is defined as the expectation value of  $H_{\Lambda}$  by the angular-momentum projected wave functions for each deformation parameter  $\beta$ ,

$$b_{\Lambda}^{\pm}(\beta) = -\langle \Psi^{0^{\pm}}(\beta) | H_{\Lambda} | \Psi^{0^{\pm}}(\beta) \rangle. \quad (14)$$

The  $b_\Lambda$  of  $0_1^+$  and  $0_1^-$  states rapidly decrease as deformation becomes larger and their behavior are quite similar to each other. As deformation becomes larger, the overlap between the wave functions of  $\Lambda$  and nucleons decreases to reduce  $V_{\Lambda N}$ . We can confirm that the 500 keV difference in  $B_\Lambda$  originates in the different deformation of  $0_1^\pm$  states from Fig. 3. This reduction of  $b_\Lambda$  as function of quadrupole deformation is qualitatively common to other  $p$ - $sd$ -shell nuclei discussed in Ref. [15, 16]. Since the  $3/2_1^-$  state is most deformed among the band head states of  $^{11}\text{Be}$ , the  $1_3^-$  state ( $^{11}\text{Be}(3/2_1^-) \otimes \Lambda_s$ ) has smallest  $B_\Lambda$ . Therefore, its excitation energy is also shifted up compared to  $^{11}\text{Be}$ . The reduction of  $B_\Lambda$  is common to other member states of  $1/2^- \otimes \Lambda_s$  and  $3/2^- \otimes \Lambda_s$  bands.

By the addition of  $\Lambda$  particle, structure of core nucleus  $^{11}\text{Be}$  is slightly modified. Due to the attraction of  $\Lambda$  particle sitting at the center of the system, the inter-cluster distance between  $2\alpha$  clusters is reduced (Fig. 2), and it leads to the reduction of the deformation and radius (Table. I). Despite of the neutron-halo structure of  $^{11}\text{Be}$ , this reduction is rather small compared to the observed case of  $^7_\Lambda\text{Li}$  [10] and cannot be clearly seen in the density distribution (Fig. 2). This is due to the presence of valence neutrons occupying molecular-orbits in  $^{12}_\Lambda\text{Be}$ . When the distance between  $2\alpha$  is reduced, the valence neutrons in  $\pi$  or  $\sigma$ -orbits lose their binding energies [22]. Therefore valence neutrons prevent drastic reduction of  $2\alpha$  distance. Note that this explains why the change of the expectation value of nuclear part is not large compared to the difference of  $B_\Lambda$ . Other interactions also predict the parity reversion of  $^{12}_\Lambda\text{Be}$ , and the mechanism is common to the case of Improved-NF. Modification of nuclear structure is not large, but the different deformation between the states leads to the difference in  $B_\Lambda$  to revert the parity of  $^{12}_\Lambda\text{Be}$ . Therefore, the predicted parity reversion of  $^{12}_\Lambda\text{Be}$  suggests a possibility to probe the different deformation between the ground and first excited states  $^{11}\text{Be}$  by adding an impurity of  $\Lambda$  particle.

Finally, we discuss the differences between three  $\Lambda N$  interactions. It was pointed out by Hiyama *et al.* [27] that YNG-ND and NF have too attractive odd-parity interaction and does not reproduce the  $B_\Lambda$  of  $^9_\Lambda\text{Be}$ . They suggested the Improved-NF introducing a repulsive short-range part in the odd-parity interaction. The difference between these  $\Lambda N$  interactions can be found in the spectrum of  $^{12}_\Lambda\text{Be}$ . We see that the  $K^\pi = 1/2^+ \otimes \Lambda_s$  and  $3/2^- \otimes \Lambda_s$  bands are located at higher excitation energies in YNG-NF and ND than Improved-NF. We remind the reader that the  $K^\pi = 1/2^-$  band of  $^{11}\text{Be}$  has 7 nucleons in  $p$ -shell, while the  $K^\pi = 1/2^+$  and  $3/2^-$  bands have 6 and 5 nucleons. Therefore, the number of the odd-parity



interactions between  $\Lambda$  and nucleons decreases for the  $1/2_1^- \otimes \Lambda_s$ ,  $1/2_1^+ \otimes \Lambda_s$  and  $3/2_1^- \otimes \Lambda_s$  bands in descending order. Consequently, when the odd-parity interaction becomes more attractive, the energy of the  $1/2_1^- \otimes \Lambda_s$  band is lowered relative to other two bands, or in other words, the  $1/2_1^+ \otimes \Lambda_s$  and  $3/2_1^- \otimes \Lambda_s$  bands are pushed up. Thus the excitation energies of the  $K^\pi = 1/2_1^+ \otimes \Lambda_s$  and  $3/2_1^- \otimes \Lambda_s$  are sensitive to the odd-parity part of  $\Lambda N$  interaction.

In summary, the low-lying states of  ${}_{\Lambda}^{12}\text{Be}$  have been investigated by the HyperAMD. We predict the parity reversion of the  ${}_{\Lambda}^{12}\text{Be}$ ; the ground state parity inverted in  ${}^{11}\text{Be}$  is reverted in  ${}_{\Lambda}^{12}\text{Be}$ . The parity reversion is caused by the different deformation of the ground and first excited states of  ${}^{11}\text{Be}$ , that produces the difference in  $B_{\Lambda}$ . This parity reversion suggests a possibility to probe the different deformation between the ground and first excited states  ${}^{11}\text{Be}$  by adding  $\Lambda$  particle as impurity. We also point out that the excitation energies of the  $K^\pi = 1/2_1^+ \otimes \Lambda_s$  and  $3/2_1^- \otimes \Lambda_s$  are sensitive to the odd-parity part of the  $\Lambda N$  interaction.

- 
- [1] M. N. Nagels, T. A. Rijken, and J. J. deSwart, Phys. Rev. D **12**, 744 (1975); D **15**, 2547 (1977); D **20**, 1633 (1979).
  - [2] Y. Yamamoto, and H. Bandō, Prog. Theor. Phys. **69**, 1312 (1983).
  - [3] D. J. Millener, A. Gal, C. Dover, and R. Dalitz, Phys. Rev. C **31**, 499 (1985).
  - [4] A. Reuver, K. Holinde, and J. Speth, Nucl. Phys. A **570**, 543 (1994).
  - [5] T. A. Rijken, and Y. Yamamoto, Phys. Rev. C **73**, 044008 (2006).
  - [6] Y. Fujiwara, Y. Suzuki, and C. Nakamoto, Prog. Part. Nucl. Phys. **58**, 439 (2007).
  - [7] A. Modragon, and E. Hernandez, Phys. Rev. C **41**, 1975 (1990).
  - [8] H. Ohkura, T. Yamada, and K. Ikeda, Prog. Theor. Phys. **94**, 47 (1995).
  - [9] E. Hiyama, M. Kamimura, K. Miyazaki, and T. Motoba, Phys. Rev. C **59**, 2351 (1999).
  - [10] K. Tanida *et al.*, Phys. Rev. Lett. **86**, 1982 (2001).
  - [11] T. Yamada, K. Ikeda, H. Bandō, and T. Motoba, Prog. Theor. Phys. **71**, 985 (1984).
  - [12] T. Sakuda, and H. Bandō, Prog. Theor. Phys. **78**, 1317 (1987).
  - [13] M. Win and K. Hagino, Phys. Rev. C **78**, 054311 (2008).
  - [14] H.-J. Schulze, M. T. Win, K. Hagino, and H. Sagawa, Prog. Theor. Phys. **123**, 569 (2010).
  - [15] M. Isaka, M. Kimura, A. Dóte, and A. Ohnishi, Phys. Rev. C **83**, 044323 (2011).
  - [16] M. Isaka, M. Kimura, A. Dóte, and A. Ohnishi, Phys. Rev. C **83**, 054304 (2011).

- [17] D. H. Wilkinson, and D. E. Alburger, Phys. Rev. **113**, 563 (1959).
- [18] I. Talmi and I. Unna, Phys. Rev. Lett. **4**, 469 (1960).
- [19] F. Ajzenberg-Selove, Nucl. Phys. A **248**, 3 (1975).
- [20] A. Dote, H. Horiuchi, and Y. Kanada-En'yo, Phys. Rev. C **56**, 1844 (1997).
- [21] Y. Kanada-En'yo, and H. Horiuchi, Phys. Rev. C **66**, 024305 (2002).
- [22] W. von Oertzen, M. Freer, and Y. Kanada-En'yo, Phys. Rep. **432**, 43 (2006), and references therein.
- [23] Y. Kanada-En'yo, M. Kimura, and H. Horiuchi, Comptes Rendus Physique **4**, 497 (2003).
- [24] M. Kimura, and H. Horiuchi, Prog. Theor. Phys. **111**, 841 (2004).
- [25] M. Kimura, Phys. Rev. C **75**, 041302 (2007).
- [26] J. Dechage, and D. Gogny, Phys. Rev. C **21**, 1568 (1980).
- [27] E. Hiyama, M. Kamimura, T. Motoba, T. Yamada, and Y. Yamamoto, Prog. Theor. Phys. **97**, 881 (1997).
- [28] D. L. Hill, and J. A. Wheeler, Phys. Rev. **89**, 1102 (1953); J. J. Griffin, and J. J. Wheeler, Phys. Rev. **108**, 311 (1957).
- [29] A. Ozawa, T. Suzuki, and I. Tanihata, Nucl. Phys. A **693**, 32 (2001).
- [30] M. Freer *et al.*, Nucl. Phys. A **834**, 621c (2010).
- [31] W. A. Peters *et al.*, Phys. Rev. C **83**, 057304 (2011).
- [32] H. T. Fortune, and R. Sherr, Phys. Rev. C **83**, 054314 (2011).